



## Mechanism underlying flow stimulation of sodium absorption in the mammalian collecting duct

Tetsuji Morimoto, Wen Liu, Craig Woda, Marcelo D. Carattino, Yuan Wei, Rebecca P. Hughey, Gerard Apodaca, Lisa M. Satlin and Thomas R. Kleyman

*Am J Physiol Renal Physiol* 291:663-669, 2006. First published Apr 25, 2006;  
doi:10.1152/ajprenal.00514.2005

**You might find this additional information useful...**

---

This article cites 45 articles, 40 of which you can access free at:

<http://ajprenal.physiology.org/cgi/content/full/291/3/F663#BIBL>

This article has been cited by 1 other HighWire hosted article:

**Airway Surface Liquid Volume Regulates ENaC by Altering the Serine Protease-Protease Inhibitor Balance: A MECHANISM FOR SODIUM HYPERABSORPTION IN CYSTIC FIBROSIS**

M. M. Myerburg, M. B. Butterworth, E. E. McKenna, K. W. Peters, R. A. Frizzell, T. R. Kleyman and J. M. Pilewski

*J. Biol. Chem.*, September 22, 2006; 281 (38): 27942-27949.

[\[Abstract\]](#) [\[Full Text\]](#) [\[PDF\]](#)

Updated information and services including high-resolution figures, can be found at:

<http://ajprenal.physiology.org/cgi/content/full/291/3/F663>

Additional material and information about *AJP - Renal Physiology* can be found at:

<http://www.the-aps.org/publications/ajprenal>

---

This information is current as of January 5, 2007 .

## Mechanism underlying flow stimulation of sodium absorption in the mammalian collecting duct

Tetsuji Morimoto,<sup>1</sup> Wen Liu,<sup>1</sup> Craig Woda,<sup>1</sup> Marcelo D. Carattino,<sup>2</sup> Yuan Wei,<sup>1</sup> Rebecca P. Hughey,<sup>2</sup> Gerard Apodaca,<sup>2</sup> Lisa M. Satlin,<sup>1</sup> and Thomas R. Kleyman<sup>2</sup>

<sup>1</sup>Division of Pediatric Nephrology, Department of Pediatrics, Mount Sinai School of Medicine, New York, New York; and <sup>2</sup>Renal Electrolyte Division, Department of Medicine, University of Pittsburgh, Pittsburgh, Pennsylvania

Submitted 21 December 2005; accepted in final form 22 March 2006

**Morimoto, Tetsuji, Wen Liu, Craig Woda, Marcelo D. Carattino, Yuan Wei, Rebecca P. Hughey, Gerard Apodaca, Lisa M. Satlin, and Thomas R. Kleyman.** Mechanism underlying flow stimulation of sodium absorption in the mammalian collecting duct. *Am J Physiol Renal Physiol* 291: F663–F669, 2006. First published April 25, 2006; doi:10.1152/ajprenal.00514.2005.—Vectorial Na<sup>+</sup> absorption across the aldosterone-sensitive distal nephron plays a key role in the regulation of extracellular fluid volume and blood pressure. Within this nephron segment, Na<sup>+</sup> diffuses from the urinary fluid into principal cells through an apical, amiloride-sensitive, epithelial Na<sup>+</sup> channel (ENaC), which is considered to be the rate-limiting step for Na<sup>+</sup> absorption. We have reported that increases in tubular flow rate in microperfused rabbit cortical collecting ducts (CCDs) lead to increases in net Na<sup>+</sup> absorption and that increases in laminar shear stress activate ENaC expressed in oocytes by increasing channel open probability. We therefore examined whether flow stimulates net Na<sup>+</sup> absorption ( $J_{Na}$ ) in CCDs by increasing channel open probability or by increasing the number of channels at the apical membrane. Both baseline and flow-stimulated  $J_{Na}$  in CCDs were mediated by ENaC, as  $J_{Na}$  was inhibited by benzamil. Flow-dependent increases in  $J_{Na}$  were observed following treatment of tubules with reagents that altered membrane trafficking by disrupting microtubules (colchicine) or Golgi (brefeldin A). Furthermore, reducing luminal Ca<sup>2+</sup> concentration ([Ca<sup>2+</sup>]) or chelating intracellular [Ca<sup>2+</sup>] with BAPTA did not prevent the flow-dependent increase in  $J_{Na}$ . Extracellular trypsin has been shown to activate ENaC by increasing channel open probability, and we observed that trypsin significantly enhanced  $J_{Na}$  when tubules were perfused at a slow flow rate. However, trypsin did not further enhance  $J_{Na}$  in CCDs perfused at fast flow rates. Similarly, the shear-induced increase in benzamil-sensitive  $J_{Na}$  in oocytes expressing protease resistance ENaC mutants was similar to that of controls. Our results suggest the rise in  $J_{Na}$  accompanying increases in luminal flow rates reflects an increase in channel open probability.

epithelial sodium channel; in vitro microperfusion; protein trafficking; mechanoregulation; laminar shear; principal cell

THE DISTAL CONVOLUTED TUBULE (DCT), connecting tubule (CNT), and collecting duct (CD) contribute to the final regulation of renal Na<sup>+</sup> reabsorption (13–16, 21, 24, 26, 28, 29, 31, 32), a process that plays a key role in modifying extracellular fluid volume and blood pressure. Within the rabbit cortical collecting duct (CCD), a segment that has been utilized extensively for functional analysis by in vitro microperfusion, Na<sup>+</sup> absorption is considered to be electrogenic and mediated by Na<sup>+</sup> diffusion from the urinary fluid into the cell through the apical amiloride-sensitive epithelial Na<sup>+</sup> channel (ENaC).

We (32, 33) and others (13, 27, 38) previously reported that increases in tubular fluid flow rate stimulate net Na<sup>+</sup> absorption in the mammalian CCD. We speculated that hydrodynamic forces associated with increases in urinary flow rate either directly activate ENaC or activate cell signaling pathways that indirectly activate ENaC. We also showed that oocytes expressing  $\alpha\beta\gamma$ -ENaC respond to increases in laminar shear stress (LSS) with a dose-dependent and reversible stimulation of benzamil-sensitive whole cell Na<sup>+</sup> currents ( $I_{Na}$ ) (9, 33). A flow-mediated increase in net Na<sup>+</sup> absorption in CCDs or  $I_{Na}$  in oocytes expressing ENaC can result from an increase in the number of apical channels and/or channel open probability. Mutant ENaC channels ( $\alpha\beta S518K\gamma$  or  $\alpha S580C\beta\gamma$  following activation with a sulfhydryl-reactive reagent) that have a high intrinsic open probability do not respond to LSS, suggesting that LSS activates ENaC by increasing channel open probability (9). We recently reported that mutations within a key region of the channel that encompasses both the selectivity filter and an amiloride-binding site affect both the rate and magnitude of channel activation in response to LSS, providing evidence that LSS induced conformational changes within the channel that affect channel gating (10).

Based on these studies, we hypothesized that the increase in net Na<sup>+</sup> absorption in the mammalian CCD that is elicited by an increase in the rate of tubular perfusion reflects ENaC activation as a result of an increase in channel open probability. To test this, we used a pharmacological approach applied to in vitro microperfused rabbit CCDs to examine the contributions of membrane trafficking and/or increases in open probability to flow stimulation of net Na<sup>+</sup> absorption. Our results suggest that flow stimulates net Na<sup>+</sup> absorption in CCDs by increasing open probability of resident Na<sup>+</sup> channels at the membrane, rather than by recruiting channels from intracellular compartments to the plasma membrane.

### METHODS

**Animals.** Adult (>6 wk) female New Zealand White rabbits obtained from Covance (Denver, PA) were housed in the Mount Sinai School of Medicine Center for Comparative Medicine. All animals were allowed free access to water and chow. Adult female *Xenopus laevis* were purchased from Xenopus Express (Plant City, FL). Animals were euthanized in accordance with National Institutes of Health *Guidelines for the Care and Use of Laboratory Animals*. Animal protocols were approved by IACUC committees at the Mount Sinai School of Medicine and the University of Pittsburgh.

The costs of publication of this article were defrayed in part by the payment of page charges. The article must therefore be hereby marked "advertisement" in accordance with 18 U.S.C. Section 1734 solely to indicate this fact.

Address for reprint requests and other correspondence: L. M. Satlin, Mount Sinai School of Medicine, One Gustave L. Levy Place, Box 1664, New York, NY 10029 (e-mail: lisa.satlin@mssm.edu).

**Microperfusion of isolated rabbit CCDs.** Kidneys were removed via a midline incision, and single tubules were dissected freehand in cold (4°C) Ringer solution containing (in mM) 135 NaCl, 2.5  $\text{K}_2\text{HPO}_4$ , 2.0  $\text{CaCl}_2$ , 1.2  $\text{MgSO}_4$ , 4.0 lactate, 6.0 L-alanine, 5.0 HEPES, and 5.5 D-glucose, pH 7.4,  $290 \pm 2$  mosmol/kg $\text{H}_2\text{O}$ , as previously described (23). A single tubule was studied from each animal.

Isolated collecting ducts were microperfused in vitro as previously described (23, 44). Briefly, each isolated tubule was immediately transferred to a temperature- and  $\text{O}_2$ - $\text{CO}_2$ -controlled specimen chamber, mounted on concentric glass pipettes, and perfused and bathed at 37°C with Burg's perfusate containing (in mM) 120 NaCl, 25  $\text{NaHCO}_3$ , 2.5  $\text{K}_2\text{HPO}_4$ , 2.0  $\text{CaCl}_2$ , 1.2  $\text{MgSO}_4$ , 4.0 Na lactate, 1.0  $\text{Na}_3$  citrate, 6.0 L-alanine, and 5.5 D-glucose, pH 7.4,  $290 \pm 2$  mosmol/kg $\text{H}_2\text{O}$  (23). During the 45-min equilibration period and thereafter, the perfusion chamber was continuously suffused with a gas mixture of 95%  $\text{O}_2$ -5%  $\text{CO}_2$  to maintain pH of the Burg's solution at 7.4 at 37°C. The bathing solution was continuously exchanged at a rate of 10 ml/h using a syringe pump (Razel, Stamford, CT).

Transport measurements were performed in the absence of transepithelial osmotic gradients, and thus water transport was assumed to be zero. Three to four samples of tubular fluid were collected under water-saturated light mineral oil by timed filling of a calibrated 30- $\mu\text{l}$  volumetric constriction pipette at each perfusion rate (slow and fast). To determine the concentration of  $\text{Na}^+$  delivered to the tubular lumen, ouabain (100  $\mu\text{M}$ ) was added to the bath at the conclusion of each experiment to inhibit all active transport, and an additional three to four samples of tubular fluid were obtained for analysis. The  $\text{Na}^+$  concentrations of perfusate and collected tubular fluid were determined by helium glow photometry and the rates of net cation transport (in  $\text{pmol} \cdot \text{min}^{-1} \cdot \text{mm tubular length}^{-1}$ ) were calculated using standard flux equations, as previously described (32). The calculated ion fluxes were averaged to obtain a single mean rate of ion transport for the CCD at each flow rate. The flow rate was varied by adjusting the height of the perfusate reservoir. The sequence of flow rates was randomized within each group of tubules to minimize any bias induced by time-dependent changes in ion transport.

In four experiments, tubular fluid collections were performed in collecting ducts perfused with Burg's solution prepared without  $\text{Ca}^{2+}$  ( $\text{Ca}^{2+}$ -free perfusate), with ( $n = 2$ ) or without ( $n = 2$ ) 100  $\mu\text{M}$  EGTA (23). In other experiments, as indicated, tubules were pretreated with luminal benzamil (5  $\mu\text{M}$ ) or trypsin (1  $\mu\text{g/ml}$ ) or basolateral lumicolchicine or colchicine (10  $\mu\text{M}$ ) (42), brefeldin A (BFA; 5  $\mu\text{g/ml}$ ) (4), or BAPTA-AM (20  $\mu\text{M}$ ). All inhibitors were added to the luminal or bathing solution, as indicated, after the 45-min equilibration period and were present for at least 30 min before tubular fluid samples were first obtained. Note that a 30-min exposure to colchicine or BFA has been reported to be effective in inhibiting microtubule function or protein trafficking from the Golgi complex to the cell membrane in distal nephron cells, respectively (22, 41, 42). Samples of tubular fluid for measurement of net  $\text{Na}^+$  absorption were collected in the continuous presence of the inhibitors.

**Oocyte expression.** cRNAs for wild-type or mutant  $\alpha$ -,  $\beta$ -, and  $\gamma$ -mENaC subunits were synthesized with T3 or T7 mMessage mMachine (Ambion, Austin, TX). Stage V-VI *Xenopus laevis* oocytes were pretreated with 1.5 mg/ml type IV collagenase and injected with 0.5–2 ng of cRNA/subunit. Injected oocytes were maintained at 18°C in modified Barth's saline [88 mM NaCl, 1 mM KCl, 2.4 mM  $\text{NaHCO}_3$ , 15 mM HEPES, 0.3 mM  $\text{Ca}(\text{NO}_3)_2$ , 0.41 mM  $\text{CaCl}_2$ , 0.82 mM  $\text{MgSO}_4$ , pH 7.4] supplemented with 10  $\mu\text{g/ml}$  sodium penicillin, 10  $\mu\text{g/ml}$  streptomycin sulfate, and 100  $\mu\text{g/ml}$  gentamicin sulfate.

**Two-electrode voltage clamp.** Two-electrode voltage clamp (TEV) was performed at 23–26°C using a GeneClamp 500B amplifier (Axon Instruments, Union City, CA). Data were acquired through Clampex 8.0 using a DigiData 1200 interface and stored on the hard disk of the computer. Pipettes filled with 3 M KCl had resistances of 0.5–5 M $\Omega$ . The extracellular solution (TEV solution) contained (in mM) 110

NaCl, 2 KCl, 1.54  $\text{CaCl}_2$ , and 10 HEPES, pH 7.4, unless indicated otherwise. In selected experiments, oocytes were pretreated with 2  $\mu\text{g/ml}$  trypsin for 5 min. The recording chamber was perfused at a rate of 3.5 ml/min. LSS was applied by perfusing TEV solution through a vertical pipette localized above the oocyte surface at a rate of 1.6 ml/min, corresponding to 0.137 dynes/cm<sup>2</sup> of shear stress as previously described (9). Bath perfusion was maintained during application of LSS. Following the stimulation process, whole cell  $\text{Na}^+$  currents were determined following bath perfusion with TEV solution supplemented with 5  $\mu\text{M}$  benzamil. The benzamil-sensitive component of the whole cell  $\text{Na}^+$  current at  $-60$  mV was used to determine ENaC-mediated whole cell  $\text{Na}^+$  current.

**Confocal immunofluorescence microscopy.** Microdissected CCDs were transferred to a petri dish containing PBS with or without colchicine (10  $\mu\text{M}$ ) or BFA (5  $\mu\text{g/ml}$ ) for 1 h and then fixed for 30 min at room temperature in PBS containing 2.5% paraformaldehyde. Fixed CCDs were rinsed in PBS three times for 5 min, blocked for 3 h at room temperature in incubation solution (1 $\times$  PBS containing 1% BSA and 0.1% Triton X-100), and then incubated overnight at 4°C with a 1:250 dilution of mouse monoclonal anti- $\alpha$  tubulin antibody (clone DM1A; Sigma) or anti-giantin antibody (gift from Adam Linstedt, Carnegie Mellon University) prepared in incubation solution. After being rinsed four times with PBS, CCDs were incubated for 80 min at room temperature with a 1:500 dilution of a fluorescein goat anti-mouse IgG (H+L) secondary antibody (Molecular Probes, Eugene, OR) prepared in incubation solution (without Triton X-100). CCDs were rinsed four times and then mounted on coverslips using Prolong Gold (Molecular Probes) mounting medium.

Imaging of immunolabeled CCDs was performed on a TCS-SL confocal microscope equipped with argon and green and red helium-neon lasers (Leica, Deerfield, IL). Images were acquired by sequential scanning using a  $\times 100$  (1.4 numerical aperture) planapochromat oil objective and the appropriate filter combination. Settings were as follows: photomultiplier set to 500–600 V, 1 Airy disk, and Kalman filter ( $n = 3$ ). Serial (z) sections were captured with a 0.30- $\mu\text{m}$  step size. The images (512  $\times$  512 pixels) were saved as TIFF files. The Volocity program (Improvision, Lexington, MA) was used to project the serial sections into one image. The contrast level of the final images was adjusted in Photoshop, and the contrast-corrected images were imported into Macromediatee FreeHand (Adobe, Mountain View, CA). Staining for tubulin and giantin was not observed in the absence of primary antibody (data not shown).

**Reagents.** Benzamil hydrochlorothiazide, trypsin, colchicine, and its inactive structural analog lumicolchicine were obtained from Sigma. Stock solutions of BFA (Calbiochem, La Jolla, CA) were prepared in DMSO and diluted 1,000-fold to yield the final concentration to which the tubule was exposed. BAPTA-AM was purchased from Molecular Probes.

**Statistics.** All results are expressed as means  $\pm$  SE;  $n$  equals the number of animal or tubule samples used for in vitro microperfusion or number of oocytes used in TEV studies. Comparisons were made by paired and unpaired  $t$ -tests as appropriate, using commercially available statistical software for the calculations (SPSS, Chicago, IL). Data comparisons among multiple groups of tubules were performed by ANOVA. Significance was asserted if  $P < 0.05$ .

## RESULTS

**Flow-stimulated  $\text{Na}^+$  absorption mediated by ENaC.** We confirmed that an increase in tubular fluid perfusion rate from  $1.1 \pm 0.1$  to  $5.3 \pm 0.3$   $\text{nl} \cdot \text{min}^{-1} \cdot \text{mm}^{-1}$  led to an increase in net  $\text{Na}^+$  absorption from  $15.4 \pm 2.6$  to  $68.5 \pm 6.9$   $\text{pmol} \cdot \text{min}^{-1} \cdot \text{mm}^{-1}$  ( $n = 9$ ;  $P < 0.001$ ; Fig. 1) and no significant change in transepithelial voltage from  $(-8.6 \pm 3.9$  to  $-3.8 \pm 2.7$  mV;  $P = \text{NS}$ ). To test whether flow-stimulated  $\text{Na}^+$  absorption is mediated by ENaC, the effect of luminal

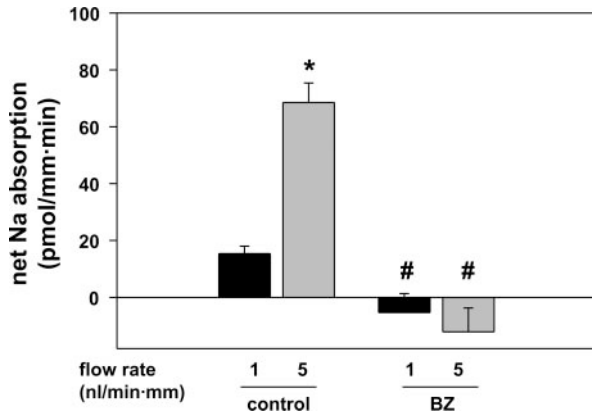


Fig. 1. Effect of benzamil (BZ) on flow-stimulated net  $\text{Na}^+$  absorption in microperfused rabbit cortical collecting ducts (CCDs). Net  $\text{Na}^+$  absorption was measured at tubular flow rates of  $\sim 1$  and  $5 \text{ nl}\cdot\text{min}^{-1}\cdot\text{mm}^{-1}$  in the absence (control;  $n = 9$ ) or presence of  $5 \mu\text{M}$  BZ ( $n = 5$ ), a selective inhibitor of epithelial sodium channels (ENaC). \* $P < 0.05$  vs. transport rate at  $1 \text{ nl}\cdot\text{min}^{-1}\cdot\text{mm}^{-1}$  in the same CCDs. # $P < 0.05$  vs. control at same flow rate.

benzamil ( $5 \mu\text{M}$ ) on flow-stimulated net  $\text{Na}^+$  absorption was measured in five rabbit CCDs (Fig. 1). Luminal benzamil completely inhibited net  $\text{Na}^+$  absorption at slow ( $-5.3 \pm 6.6 \text{ pmol}\cdot\text{min}^{-1}\cdot\text{mm}^{-1}$  at  $1.0 \pm 0.1 \text{ nl}\cdot\text{min}^{-1}\cdot\text{mm}^{-1}$ ) and fast ( $-12.1 \pm 8.4 \text{ pmol}\cdot\text{min}^{-1}\cdot\text{mm}^{-1}$  at  $4.4 \text{ nl}\cdot\text{min}^{-1}\cdot\text{mm}^{-1}$ ) flow rates ( $P < 0.05$  compared with control CCDs). Transepithelial voltage in the benzamil-treated CCDs was  $3.0 \pm 0.9$  and  $2.4 \pm 1.0 \text{ mV}$  at the two flow rates [ $P =$  not significant (NS)], respectively. These data suggest that a benzamil-sensitive pathway, presumably ENaC, mediates both basal and flow-stimulated net  $\text{Na}^+$  absorption in mammalian CCDs.

Flow-induced increases in net  $\text{Na}^+$  transport do not require an increase in intracellular  $\text{Ca}^{2+}$  concentration. We previously showed that increases in the rate of tubular perfusion are associated with a large transient high peak and lower sustained elevation in intracellular  $\text{Ca}^{2+}$  concentration ( $[\text{Ca}^{2+}]_i$ ) in principal cells as well as intercalated cells (23, 43, 44). Although large increases in  $[\text{Ca}^{2+}]_i$  are predicted to inhibit ENaC at the plasma membrane (30, 36), more modest increases in  $[\text{Ca}^{2+}]_i$  might facilitate exocytic insertion of channels from an intracellular pool into the plasma membrane (8, 45). To determine whether luminal  $\text{Ca}^{2+}$  entry and the consequent rise in  $[\text{Ca}^{2+}]_i$  associated with high tubular flow rates in the CCD are required for flow-stimulated net  $\text{Na}^+$  absorption, isolated tubules were perfused in the absence of luminal  $\text{Ca}^{2+}$  (either with or without luminal EGTA) or after loading with the permeant intracellular  $\text{Ca}^{2+}$  chelator BAPTA-AM ( $20 \mu\text{M}$ ). We previously showed that removal of luminal  $\text{Ca}^{2+}$  does not affect resting  $[\text{Ca}^{2+}]_i$  but markedly attenuates the flow-induced rise in  $[\text{Ca}^{2+}]_i$  (23).

In the absence of luminal  $\text{Ca}^{2+}$ , an increase in flow rate from  $1.0 \pm 0.2$  to  $5.7 \pm 0.2 \text{ nl}\cdot\text{min}^{-1}\cdot\text{mm}^{-1}$  induced a significant increase in net  $\text{Na}^+$  absorption from  $12.9 \pm 2.6$  to  $63.1 \pm 16.9 \text{ pmol}\cdot\text{min}^{-1}\cdot\text{mm}^{-1}$  ( $P < 0.05$ ;  $n = 4$ ; Fig. 2), indicating that flow stimulation of net  $\text{Na}^+$  absorption does not require luminal  $\text{Ca}^{2+}$  entry. Similarly, chelation of  $[\text{Ca}^{2+}]_i$  did not inhibit flow stimulation of net  $\text{Na}^+$  absorption. An increase in flow rate from  $1.4 \pm 0.3$  to  $5.4 \pm 0.1 \text{ nl}\cdot\text{min}^{-1}\cdot\text{mm}^{-1}$  in BAPTA-loaded CCDs induced a significant increase in net  $\text{Na}^+$  absorption from  $10.1 \pm 3.1$  to  $48.6 \pm 6.3 \text{ pmol}\cdot\text{min}^{-1}\cdot\text{mm}^{-1}$  ( $P < 0.05$ ;  $n = 3$ ; Fig. 2).

Flow-induced increases in net  $\text{Na}^+$  absorption reflect an increase in channel open probability. Microtubule-dependent vesicle transport plays an important role in specific membrane trafficking events, including exocytosis (17). To test whether the flow-induced increase in net  $\text{Na}^+$  absorption requires intact microtubule function, CCDs were incubated with  $10 \mu\text{M}$  colchicine ( $n = 6$ ) or the inactive analog lumicolchicine ( $n = 4$ ) for 1 h and the effect of an increase in luminal flow rate on net  $\text{Na}^+$  absorption was measured in the continued presence of the agent. Localization of tubulin with a monoclonal antitubulin antibody demonstrated that the microtubular architecture was disrupted in colchicine-treated tubules (Fig. 3, A and B). An increase in luminal flow rate in colchicine-treated CCDs from  $1.0 \pm 0.2$  to  $4.5 \pm 0.3 \text{ nl}\cdot\text{min}^{-1}\cdot\text{mm}^{-1}$  was associated with an increase in net  $\text{Na}^+$  absorption from  $14.7 \pm 3.8$  to  $41.8 \pm 6.5 \text{ pmol}\cdot\text{min}^{-1}\cdot\text{mm}^{-1}$  ( $P < 0.01$ ; Fig. 4), an increase similar to that detected in untreated control and lumicolchicine-treated ( $n = 4$ ) CCDs perfused at similar flow rates ( $P =$  NS; Fig. 4). These results suggest that flow activation of ENaC is not dependent on intact microtubules.

To further explore whether an increase in luminal flow rate stimulates trafficking of newly synthesized channels from the *trans*-Golgi network to the plasma membrane, we examined the effect of BFA ( $5 \mu\text{g/ml}$ ) on flow-stimulated net  $\text{Na}^+$  absorption in the CCD ( $n = 4$ ). BFA treatment results in an inhibition of delivery of channels from the intracellular pool to the plasma membrane (4, 11). If ENaC activation by flow is dependent on exocytic insertion of channels into the plasma membrane, BFA treatment should block the flow-dependent increase in net  $\text{Na}^+$  absorption. We observed that net  $\text{Na}^+$  absorption increased from  $12.2 \pm 3.4$  to  $32.4 \pm 8.5 \text{ pmol}\cdot\text{min}^{-1}\cdot\text{mm}^{-1}$  ( $P < 0.05$ ) in BFA-treated tubules as the tubular flow rate was increased from  $1.0 \pm 0.1$  to  $5.0 \pm 0.3 \text{ nl}\cdot\text{min}^{-1}\cdot\text{mm}^{-1}$  (Fig. 4). Net  $\text{Na}^+$  absorption in BFA-treated CCDs did not significantly differ from that measured in untreated control, lumicolchicine-, and colchicine-treated CCDs perfused at the slow and fast flow rates in this set of experiments ( $P =$  NS). While protein trafficking to plasma mem-

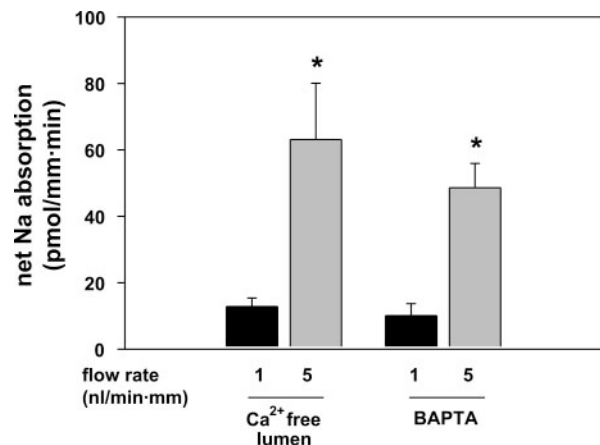


Fig. 2. Effect of removal of luminal  $\text{Ca}^{2+}$  ( $\text{Ca}^{2+}$ -free perfusate) or intracellular  $\text{Ca}^{2+}$  chelation on flow-stimulated net  $\text{Na}^+$  absorption in microperfused rabbit CCDs. Net  $\text{Na}^+$  absorption was measured at tubular flow rates of  $\sim 1$  and  $5 \text{ nl}\cdot\text{min}^{-1}\cdot\text{mm}^{-1}$  in the absence of luminal  $\text{Ca}^{2+}$  ( $\pm$  EGTA, as indicated in METHODS;  $n = 4$ ) or presence of  $20 \mu\text{M}$  BAPTA-AM, a chelator of intracellular  $\text{Ca}^{2+}$  ( $n = 3$ ). \* $P < 0.05$  vs. transport rate at  $1 \text{ nl}\cdot\text{min}^{-1}\cdot\text{mm}^{-1}$  in the same CCDs.

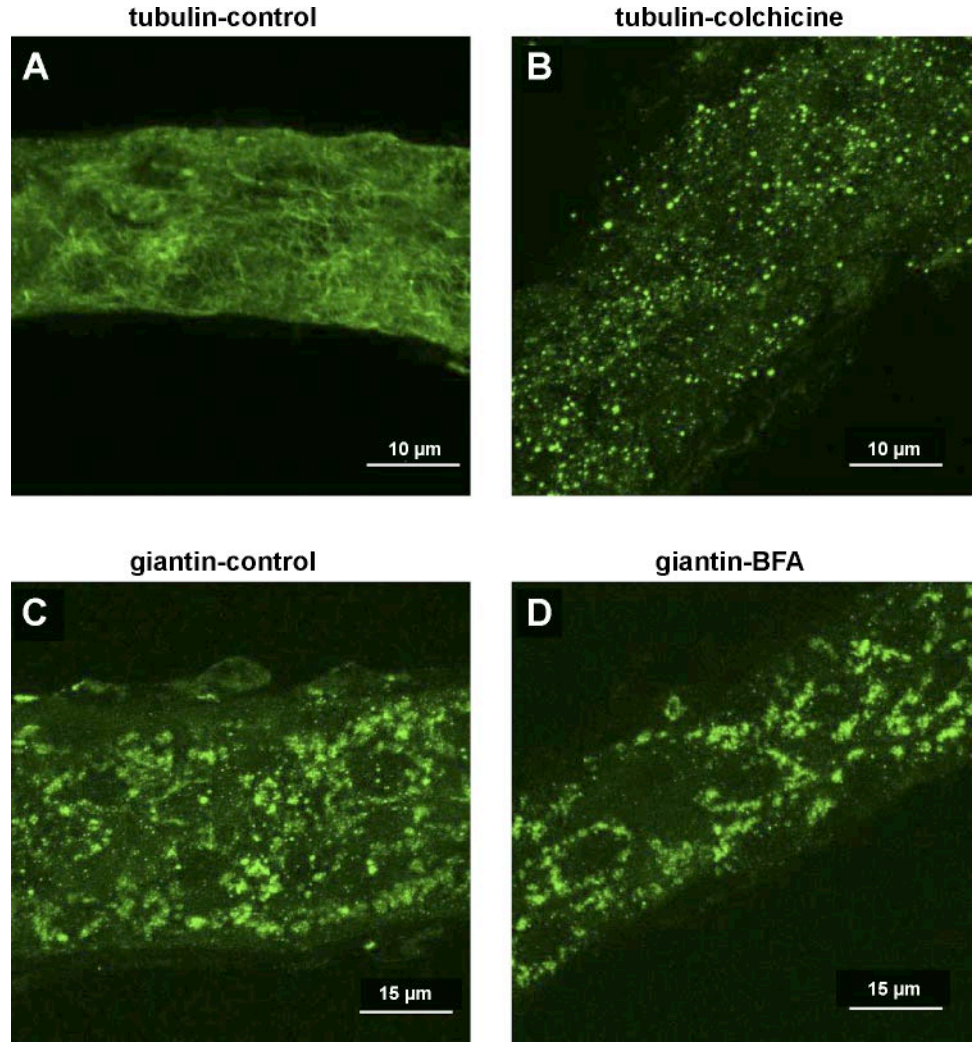


Fig. 3. Effect of colchicine and brefeldin A (BFA) on microtubular and Golgi architecture. Isolated rabbit CCDs were treated with 10  $\mu$ M colchicine, 5  $\mu$ g/ml BFA, or vehicle alone for 1 h and then fixed. Microtubules were localized with a monoclonal anti-tubulin antibody in control (A) and colchicine-treated (B) CCDs. Giantin, a Golgi marker, was localized with a monoclonal anti-giantin antibody in control (C) and BFA-treated (D) CCDs.

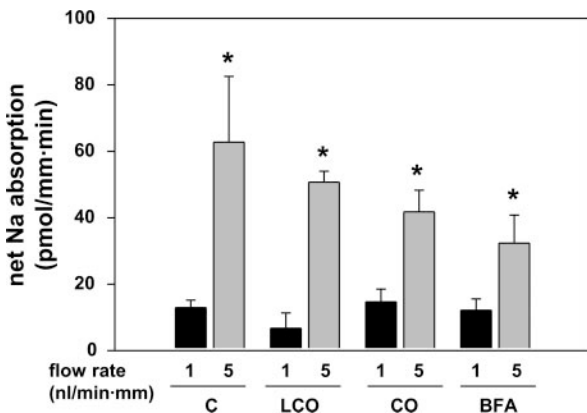


Fig. 4. Effect of lumicolchicine (LCO), colchicine (CO), and BFA on flow-stimulated net Na<sup>+</sup> absorption in microperfused rabbit CCDs. Net Na<sup>+</sup> absorption was measured at tubular flow rates of  $\sim$ 1 and 5  $\text{nl}\cdot\text{min}^{-1}\cdot\text{mm}^{-1}$  in the absence (C for control;  $n = 4$ ) or presence of 10  $\mu$ M colchicine ( $n = 6$ ), a microtubule inhibitor, the same concentration of its inactive structural analog LCO ( $n = 4$ ), or 5  $\mu$ g/ml BFA ( $n = 4$ ), an agent that disrupts Golgi and inhibits delivery of channels from the intracellular pool to the plasma membrane (4, 35). \* $P < 0.05$  vs. transport rate at 1  $\text{nl}\cdot\text{min}^{-1}\cdot\text{mm}^{-1}$  in the same CCDs.

branes has been reported to be sensitive to BFA, some cells have been shown to be relatively resistant to the disruption of Golgi architecture by BFA (3, 25). In fact, we observed that the perinuclear localization of giantin, a Golgi marker, was similar in control and BFA-treated tubules (Fig. 3, C and D). A lack of effect of low concentrations of BFA, sufficient to disrupt trafficking to the plasma membrane in Madin-Darby canine kidney (MDCK) and mouse CCD cells, on the distribution of selected Golgi markers has been observed in MDCK cells (3, 4, 25).

Recent studies suggest that ENaC extracellular domains are processed by proteases (18, 20). Channels that have not been processed by proteases appear to have a very low open probability (7, 18, 34). Furthermore, channels with an intrinsically low open probability respond to external trypsin with a dramatic increase in channel open probability, such that channels exhibit “normal” gating behavior with characteristically long open and closed times (7, 34). If both flow and trypsin-dependent proteolysis activate ENaC by increasing channel open probability, the effects of flow and trypsin on net Na<sup>+</sup> absorption might not be additive. We first measured net Na<sup>+</sup> absorption at a slow tubular flow rate before and after luminal perfusion with trypsin (1  $\mu$ g/ml). At a slow flow rate of  $1.3 \pm 0.2 \text{ nl}\cdot\text{min}^{-1}\cdot\text{mm}^{-1}$ , the rate of net Na<sup>+</sup> absorption in trypsin-

treated CCDs ( $25.8 \pm 3.0 \text{ pmol} \cdot \text{min}^{-1} \cdot \text{mm}^{-1}$ ;  $n = 5$ ) significantly exceeded that measured in control tubules ( $15.4 \pm 2.6$ ,  $n = 9$ ;  $P = 0.03$ ; Fig. 5), consistent with protease activation of resident ENaCs in the apical membrane. However, trypsin did not alter the rate of net  $\text{Na}^+$  absorption measured at fast flow rates ( $68.5 \pm 6.9 \text{ pmol} \cdot \text{min}^{-1} \cdot \text{mm}^{-1}$  at  $5.3 \pm 0.3 \text{ nl} \cdot \text{min}^{-1} \cdot \text{mm}^{-1}$  in the absence of trypsin vs.  $76.3 \pm 7.3 \text{ pmol} \cdot \text{min}^{-1} \cdot \text{mm}^{-1}$  at  $5.7 \pm 0.4 \text{ nl} \cdot \text{min}^{-1} \cdot \text{mm}^{-1}$  in the presence of trypsin;  $P = 0.48$ ; Fig. 5). In CCDs pretreated with trypsin, the  $3.2 \pm 0.6$ -fold increase in net  $\text{Na}^+$  absorption elicited by an increase in tubular flow rate was significantly lower than the  $5.9 \pm 1.6$ -fold increase observed in control CCDs ( $P < 0.05$ ).

*Flow activates channels that have not been processed by proteases.* Our previous observations, as well as work from other groups, suggest that both noncleaved channels as well as channels that have been processed by proteases are expressed at the apical plasma membrane of epithelia (2, 6, 19, 20). Channels that have not been processed by proteases respond to trypsin with a large increase in open probability (6, 7, 18). Our observation that trypsin treatment did not significantly enhance the rate of  $\text{Na}^+$  absorption under high-flow conditions raised the possibility that noncleaved channels are activated by flow. We previously showed that ENaCs with mutations at key sites in the  $\alpha$  [RtripleA (R205A/R028A/R231A)] and  $\gamma$  (R143A) subunits are not processed by proteases in oocytes (18). We examined whether  $\alpha\text{RtripleA}\beta\gamma\text{R143A}$  channels expressed in oocytes were activated by LSS, which was generated by perfusing TEV solution through a vertical pipette localized above the oocyte surface at a rate of 1.6 ml/min, corresponding to  $0.137 \text{ dynes/cm}^2$  of shear stress. The fold-increase in benzamil ( $5 \mu\text{M}$ )-sensitive whole cell  $\text{Na}^+$  currents ( $I_{\text{Na}}$ ) in oocytes expressing  $\alpha\text{RtripleA}\beta\gamma\text{R143A}$  in response to LSS was  $0.38 \pm 0.05$ -fold ( $n = 14$ ; Fig. 6), nearly identical to the  $0.36 \pm 0.04$ -fold ( $n = 16$ ) increase in  $I_{\text{Na}}$  observed in oocytes expressing wild-type ENaC ( $P = 0.72$ , unpaired  $t$ -test).

*Flow activates channels that have been processed by proteases.* Net  $\text{Na}^+$  absorption in trypsin-treated CCDs perfused at slow flow rates ( $25.8 \pm 3.0 \text{ pmol} \cdot \text{min}^{-1} \cdot \text{mm}^{-1}$ ;  $n = 5$ ) was significantly less than that measured at fast flow rates ( $76.3 \pm$

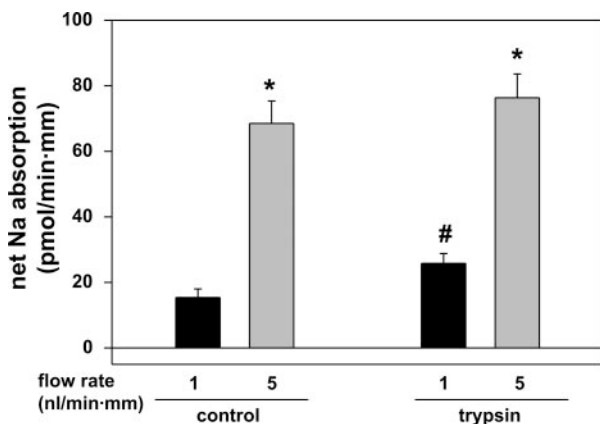


Fig. 5. Effect of trypsin on flow-stimulated net  $\text{Na}^+$  absorption in microperfused rabbit CCDs. Net  $\text{Na}^+$  absorption was measured at tubular flow rates of  $\sim 1$  and  $5 \text{ nl} \cdot \text{min}^{-1} \cdot \text{mm}^{-1}$  in the absence (control;  $n = 9$ ) or presence of  $1 \mu\text{g/ml}$  trypsin ( $n = 5$ ), which increases the open probability of the channel (7, 12, 18). \* $P < 0.05$  vs. transport rate at  $1 \text{ nl} \cdot \text{min}^{-1} \cdot \text{mm}^{-1}$  in the same CCDs. # $P < 0.05$  vs. control at same flow rate.

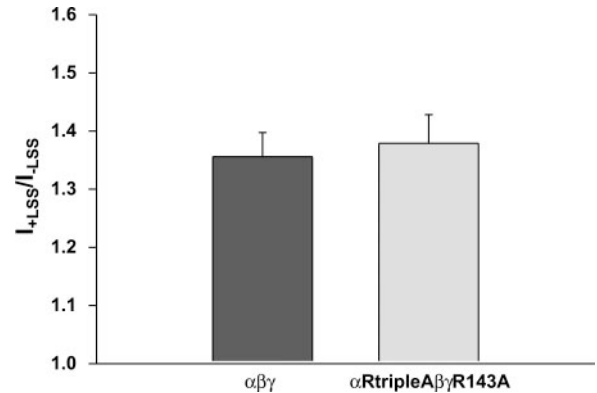


Fig. 6. Effect of laminar shear stress (LSS) on whole cell  $\text{Na}^+$  currents in oocytes expressing noncleaved ENaC channels ( $\alpha\text{R205A/R208A/R231A}\beta\gamma\text{R143A}$ ). Oocytes were injected with cRNAs for wild-type  $\alpha\beta\gamma$  or for  $\alpha\text{RtripleA}\beta\gamma\text{R143A}$ . The  $\alpha$ - and  $\gamma$ -subunits had a  $\text{NH}_2$ -terminal HA and  $\text{COOH}$ -terminal V5 tags. The fold-increase in benzamil ( $5 \mu\text{M}$ )-sensitive whole cell  $\text{Na}^+$  currents ( $I_{\text{Na}}$ ) in oocytes expressing wild-type ENaC ( $n = 16$ ) or  $\alpha\text{RtripleA}\beta\gamma\text{R143A}$  ( $n = 14$ ) was measured in response to a LSS rate of  $0.137 \text{ dynes/cm}^2$ .

$7.3 \text{ pmol} \cdot \text{min}^{-1} \cdot \text{mm}^{-1}$ ;  $n = 5$ ,  $P < 0.01$ ). These results suggest that flow activates channels that have been previously activated by proteases. We therefore examined whether wild-type channels expressed in oocytes, following trypsin treatment, were activated by LSS. The fold-increase in benzamil ( $5 \mu\text{M}$ )-sensitive whole cell  $I_{\text{Na}}$  in oocytes expressing wild-type channels in response to LSS was  $0.37 \pm 0.07$ -fold ( $n = 8$ ; Fig. 7), similar to the  $0.52 \pm 0.13$ -fold ( $n = 6$ ) increase in  $I_{\text{Na}}$  observed in oocytes expressing wild-type ENaC that were pretreated with trypsin ( $P = 0.31$ , unpaired  $t$ -test). Our results suggest that the open probability of protease-activated channels can be further increased by LSS.

DISCUSSION

Renal epithelial cells in the distal nephron are subject to continuous variations in urinary flow rate. We previously reported that an increase in luminal flow rate from 1 to  $\sim 5 \text{ nl} \cdot \text{min}^{-1} \cdot \text{mm}^{-1}$  stimulates net  $\text{Na}^+$  absorption as well as

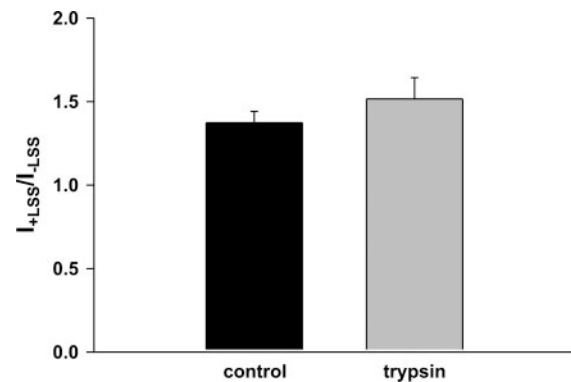


Fig. 7. Effect of trypsin on LSS-induced increase in whole cell  $\text{Na}^+$  currents in oocytes expressing wild-type ENaC. Oocytes were injected with cRNAs for wild-type  $\alpha\beta\gamma$  ENaC. LSS was generated as described in METHODS. The extracellular solution contained (in mM) 110 Na gluconate, 1.54  $\text{CaCl}_2$ , 2  $\text{BaCl}_2$ , 10 tetraethylammonium chloride, and 10 HEPES, pH 7.4. The fold-increase in benzamil ( $5 \mu\text{M}$ )-sensitive whole cell  $I_{\text{Na}}$  in ENaC-expressing oocytes studied in the absence ( $n = 8$ ) or presence of trypsin ( $2 \mu\text{g/ml}$ ;  $n = 6$ ) was measured in response to a LSS rate of  $0.137 \text{ dynes/cm}^2$ .

$\text{K}^+$  secretion (32, 33, 44). The purpose of the present study was to confirm that flow-stimulated net  $\text{Na}^+$  absorption is mediated by ENaC and, if so, examine whether the flow-dependent activation of  $\text{Na}^+$  transport reflects an increase in open probability or density of apical resident ENaCs in the mammalian CCD.

The observation that benzamil inhibited net  $\text{Na}^+$  absorption both at slow and fast flow rates (Fig. 1) is consistent with a major role of ENaC in mediating flow-stimulated net  $\text{Na}^+$  absorption. ENaC activity can be regulated by two distinct mechanisms: changes in open probability of channels resident at the apical membrane or changes in the number of apical conducting channels due to recruitment of ENaCs from subapical storage pools (37). We previously showed that a rapid increase in luminal flow rate in the microperfused rabbit CCD elicits an increase in  $[\text{Ca}^{2+}]_i$  that reflects both release of  $\text{Ca}^{2+}$  from internal, phosphoinositol-sensitive stores and external  $\text{Ca}^{2+}$  entry, processes that are mutually dependent on each other (23). Although increases in  $[\text{Ca}^{2+}]_i$  might increase ENaC activity by enhancing the trafficking of ENaC channels from an intracellular pool to the plasma membrane, Palmer et al. (30, 36) suggested that increases in  $[\text{Ca}^{2+}]_i$  from basal levels to concentrations  $>500$  nM inhibit ENaC activity by reducing channel open probability. The effect of modest increases in  $[\text{Ca}^{2+}]_i$  noted in response to an increase in flow on  $\text{Na}^+$  channel open probability is not known. Our studies demonstrate that flow-dependent increases in ENaC activity are not dependent on increases in  $[\text{Ca}^{2+}]_i$  (Fig. 2). We observed flow-dependent increases in net  $\text{Na}^+$  absorption in tubules pretreated with BAPTA to chelate intracellular  $\text{Ca}^{2+}$ , as well as tubules perfused with a luminal buffer nominally free of  $\text{Ca}^{2+}$ .

Acute stimulation of ENaC in  $\text{Na}^+$  absorptive epithelia by forskolin (or cAMP) is mediated by channel recruitment to the apical membrane from a subapical vesicle-based recycling pool (4). Both colchicine, which disrupts microtubules, as well as BFA, which disrupts Golgi and inhibits antegrade trafficking from the TGN to the apical membrane, prevented forskolin-stimulated increases in ENaC activity in cultured CCD cells (4, 5). In contrast, we observed flow-dependent increases in net  $\text{Na}^+$  absorption in CCDs treated with either colchicine or BFA (Fig. 4), suggesting that flow-dependent activation of ENaC is not due recruitment of channels from an intracellular pool to the plasma membrane.

ENaC open probability is regulated by a number of factors. Recent studies suggest that proteolytic processing of ENaC subunits by proteases, including furin, prostatin, and other serine proteases, activates ENaC by increasing channel open probability (1, 6, 7, 18, 39, 40). Channel activation by proteases appears to be associated with a conversion of channels that have a very low open probability, referred to as "near-silent channels," to channels that exhibit "normal" gating behavior with long mean open and closed times (7). Analysis of the effects of trypsin on flow-stimulated  $\text{Na}^+$  absorption provides insight into mechanisms mediating flow-dependent increases in net  $\text{Na}^+$  absorption. We noted that net  $\text{Na}^+$  absorption in trypsin-treated CCDs perfused at a slow luminal flow rate of  $\sim 1 \text{ nl} \cdot \text{min}^{-1} \cdot \text{mm}^{-1}$  was approximately twice that measured in control (non-trypsin-treated) CCDs perfused at the same flow rate (Fig. 5). This result is consistent with a protease-mediated increase in open probability of resident

channels and suggests that a sizeable pool of noncleaved channels is present at the CCD plasma membrane. We also observed that  $\text{Na}^+$  absorption in trypsin-treated CCDs at slow flow rates was significantly less than that observed in trypsin-treated CCDs at high flow rates. Furthermore,  $\text{Na}^+$  currents measured in oocytes expressing wild-type ENaC that were pretreated with trypsin increase in response to laminar shear. These results suggest that flow activates channels that have been previously activated by proteases. In contrast, when tubular segments were perfused at fast flow rates, a significant enhancement of net  $\text{Na}^+$  absorption was not observed following trypsin treatment. We interpret these results to indicate that 1) flow stimulation of net  $\text{Na}^+$  absorption is predominantly due to an increase in ENaC open probability and 2) both noncleaved and cleaved channels are activated by flow. We observed that the fold-increase in whole cell  $\text{Na}^+$  currents in oocytes expressing noncleaved channels ( $\alpha\text{R205A/R208A/R231A}\beta\gamma\text{R143A}$ ) in response to LSS was similar that observed in oocytes expressing wild-type channels (Fig. 5). These data provide additional evidence that noncleaved channels are activated by flow.

In summary, our results suggest that increases in tubular flow rates activate ENaC primarily by increasing channel open probability. Once channels are activated by flow, they do not exhibit further activation in response to proteases. Although the mechanisms by which ENaC senses mechanical forces in the distal nephron have not been elucidated, we propose that variations in flow rates in the distal nephron induce conformational changes in the channel's gate that alter channel open probability (10).

#### ACKNOWLEDGMENTS

The authors gratefully acknowledge B. Zamilovitz and W. G. Ruiz for excellent technical support. We thank A. Linstedt (Carnegie Mellon University) for providing the antigiantin antibody.

Abstracts of this work were presented at the American Society of Nephrology Renal Week 2004 (St. Louis, MO) and Renal Week 2005 (Philadelphia, PA).

#### GRANTS

This work was supported by National Institutes of Health Grants DK-038470 (to L. M. Satlin), DK-051391 (to T. R. Kleyman), and DK-054425 (to G. Apodaca). T. Morimoto was supported by a Kidney and Urology Foundation of America Fellowship grant, W. Liu by a PKD Foundation Fellowship grant, and Y. Wei by an American Heart Association Scientist Development grant.

#### REFERENCES

- Adachi M, Kitamura K, Miyoshi T, Narikiyo T, Iwashita K, Shiraishi N, Nonoguchi H, and Tomita K. Activation of epithelial sodium channels by prostatin in *Xenopus* oocytes. *J Am Soc Nephrol* 12: 1114–1121, 2001.
- Alvarez de la Rosa D, Li H, and Canessa CM. Effects of aldosterone on biosynthesis, traffic, and functional expression of epithelial sodium channels in A6 cells. *J Gen Physiol* 119: 427–442, 2002.
- Apodaca G, Aroeti B, Tang K, and Mostov KE. Brefeldin-A inhibits the delivery of the polymeric immunoglobulin receptor to the basolateral surface of MDCK cells. *J Biol Chem* 268: 20380–20385, 1993.
- Butterworth MB, Edinger RS, Johnson JP, and Frizzell RA. Acute ENaC stimulation by cAMP in a kidney cell line is mediated by exocytic insertion from a recycling channel pool. *J Gen Physiol* 125: 81–101, 2005.
- Butterworth MB, Edinger RS, Johnson JP, and Frizzell RA. Cytoskeletal involvement in cAMP mediated ENaC regulation. *FASEB J* 19: A1177, 2005.
- Caldwell RA, Boucher RC, and Stutts MJ. Neutrophil elastase activates near-silent epithelial  $\text{Na}^+$  channels and increases airway epithelial  $\text{Na}^+$  transport. *Am J Physiol Lung Cell Mol Physiol* 288: L813–L819, 2005.

7. **Caldwell RA, Boucher RC, and Stutts MJ.** Serine protease activation of near-silent epithelial  $\text{Na}^+$  channels. *Am J Physiol Cell Physiol* 286: C190–C194, 2004.
8. **Cannon C, van Adelsberg J, Kelly S, and Al-Awqati Q.** Carbon-dioxide-induced exocytotic insertion of  $\text{H}^+$  pumps in turtle-bladder luminal membrane: role of cell pH and calcium. *Nature* 314: 443–446, 1985.
9. **Carattino MD, Sheng S, and Kleyman TR.** Epithelial  $\text{Na}^+$  channels are activated by laminar shear stress. *J Biol Chem* 279: 4120–4126, 2004.
10. **Carattino MD, Sheng S, and Kleyman TR.** Mutations in the pore region modify epithelial sodium channel gating by shear stress. *J Biol Chem* 280: 4393–4401, 2005.
11. **Chardin P and McCormick F.** Brefeldin A: the advantage of being uncompetitive. *Cell* 97: 153–155, 1999.
12. **Chraïbi A, Vallet V, Firsov D, Hess SK, and Horisberger JD.** Protease modulation of the activity of the epithelial sodium channel expressed in *Xenopus* oocytes. *J Gen Physiol* 111: 127–138, 1998.
13. **Engbretson BG and Stoner LC.** Flow-dependent potassium secretion by rabbit cortical collecting tubule in vitro. *Am J Physiol Renal Fluid Electrolyte Physiol* 253: F896–F903, 1987.
14. **Giebisch G.** Renal potassium transport: mechanisms and regulation. *Am J Physiol Renal Physiol* 274: F817–F833, 1998.
15. **Good DW and Wright FS.** Luminal influences on potassium secretion: sodium concentration and fluid flow rate. *Am J Physiol Renal Fluid Electrolyte Physiol* 236: F192–F205, 1979.
16. **Grantham JJ, Burg MB, and Orloff J.** The nature of transtubular Na and K transport in isolated rabbit renal collecting tubules. *J Clin Invest* 49: 1815–1826, 1970.
17. **Hamm-Alvarez SF and Sheetz MP.** Microtubule-dependent vesicle transport: modulation of channel and transporter activity in liver and kidney. *Physiol Rev* 78: 1109–1129, 1998.
18. **Hughey RP, Bruns JB, Kinlough CL, Harkleroad KL, Tong Q, Carattino MD, Johnson JP, Stockand JD, and Kleyman TR.** Epithelial sodium channels are activated by furin-dependent proteolysis. *J Biol Chem* 279: 18111–18114, 2004.
19. **Hughey RP, Bruns JB, Kinlough CL, and Kleyman TR.** Distinct pools of epithelial sodium channels are expressed at the plasma membrane. *J Biol Chem* 279: 48491–48494, 2004.
20. **Hughey RP, Mueller GM, Bruns JB, Kinlough CL, Poland PA, Harkleroad KL, Carattino MD, and Kleyman TR.** Maturation of the epithelial  $\text{Na}^+$  channel involves proteolytic processing of the alpha- and gamma-subunits. *J Biol Chem* 278: 37073–37082, 2003.
21. **Imai M and Nakamura R.** Function of distal convoluted and connecting tubules studied by isolated nephron segments. *Kidney Int* 22: 465–472, 1982.
22. **Kleyman TR, Ernst SA, and Coupaye-Gerard B.** Arginine vasopressin and forskolin regulate apical cell surface expression of epithelial  $\text{Na}^+$  channels in A6 cells. *Am J Physiol Renal Fluid Electrolyte Physiol* 266: F506–F511, 1994.
23. **Liu W, Xu S, Woda C, Kim P, Weinbaum S, and Satlin LM.** Effect of flow and stretch on the  $[\text{Ca}^{2+}]_i$  response of principal and intercalated cells in cortical collecting duct. *Am J Physiol Renal Physiol* 285: F998–F1012, 2003.
24. **Loffing J, Pietri L, Aregger F, Bloch-Faure M, Ziegler U, Meneton P, Rossier BC, and Kaissling B.** Differential subcellular localization of ENaC subunits in mouse kidney in response to high- and low-Na diets. *Am J Physiol Renal Physiol* 279: F252–F258, 2000.
25. **Low SH, Wong SH, Tang BL, Tan P, Subramaniam VN, and Hong W.** Inhibition by brefeldin A of protein secretion from the apical cell surface of Madin-Darby canine kidney cells. *J Biol Chem* 266: 17729–17732, 1991.
26. **Madsen KM and Tisher CC.** Structural-functional relationship along the distal nephron. *Am J Physiol Renal Fluid Electrolyte Physiol* 250: F1–F15, 1986.
27. **Malnic G, Berliner RW, and Giebisch G.** Flow dependence of  $\text{K}^+$  secretion in cortical distal tubules of the rat. *Am J Physiol Renal Fluid Electrolyte Physiol* 256: F932–F941, 1989.
28. **Malnic G, Klose RM, and Giebisch G.** Microperfusion study of distal tubular potassium and sodium transfer in rat kidney. *Am J Physiol* 211: 548–559, 1966.
29. **Malnic G, Klose RM, and Giebisch G.** Micropuncture study of distal tubular potassium and sodium transport in rat nephron. *Am J Physiol* 211: 529–547, 1966.
30. **Palmer LG and Frindt G.** Effects of cell Ca and pH on Na channels from rat cortical collecting tubule. *Am J Physiol Renal Fluid Electrolyte Physiol* 253: F333–F339, 1987.
31. **Rubera I, Loffing J, Palmer LG, Frindt G, Fowler-Jaeger N, Sauter D, Carroll T, McMahon A, Hummler E, and Rossier BC.** Collecting duct-specific gene inactivation of alphaENaC in the mouse kidney does not impair sodium and potassium balance. *J Clin Invest* 112: 554–565, 2003.
32. **Satlin LM.** Postnatal maturation of potassium transport in rabbit cortical collecting duct. *Am J Physiol Renal Fluid Electrolyte Physiol* 266: F57–F65, 1994.
33. **Satlin LM, Sheng S, Woda CB, and Kleyman TR.** Epithelial  $\text{Na}^+$  channels are regulated by flow. *Am J Physiol Renal Physiol* 280: F1010–F1018, 2001.
34. **Sheng S, Carattino MD, Bruns JB, Hughey RP, and Kleyman TR.** Furin cleavage activates the epithelial  $\text{Na}^+$  channels by relieving  $\text{Na}^+$  self-inhibition. *Am J Physiol Renal Physiol* 290: F1488–F1496, 2006.
35. **Shimkets RA, Lifton RP, and Canessa CM.** The activity of the epithelial sodium channel is regulated by clathrin-mediated endocytosis. *J Biol Chem* 272: 25537–25541, 1997.
36. **Silver RB, Frindt G, Windhager EE, and Palmer LG.** Feedback regulation of Na channels in rat CCT. I. Effects of inhibition of Na pump. *Am J Physiol Renal Fluid Electrolyte Physiol* 264: F557–F564, 1993.
37. **Snyder PM.** The epithelial  $\text{Na}^+$  channel: cell surface insertion and retrieval in  $\text{Na}^+$  homeostasis and hypertension. *Endocr Rev* 23: 258–275, 2002.
38. **Stokes JB.** Ion transport by the collecting duct. *Semin Nephrol* 13: 202–212, 1993.
39. **Vuagniaux G, Vallet V, Jaeger NF, Hummler E, and Rossier BC.** Synergistic activation of ENaC by three membrane-bound channel-activating serine proteases (mCAP1, mCAP2, and mCAP3) and serum- and glucocorticoid-regulated kinase (Sgk1) in *Xenopus* oocytes. *J Gen Physiol* 120: 191–201, 2002.
40. **Vuagniaux G, Vallet V, Jaeger NF, Pfister C, Bens M, Farman N, Courtois-Coutry N, Vandewalle A, Rossier BC, and Hummler E.** Activation of the amiloride-sensitive epithelial sodium channel by the serine protease mCAP1 expressed in a mouse cortical collecting duct cell line. *J Am Soc Nephrol* 11: 828–834, 2000.
41. **Wei Y, Bloom P, Gu R, and Wang W.** Protein-tyrosine phosphatase reduces the number of apical small conductance  $\text{K}^+$  channels in the rat cortical collecting duct. *J Biol Chem* 275: 20502–20507, 2000.
42. **Wei Y and Wang WH.** Role of the cytoskeleton in mediating effect of vasopressin and herbimycin A on secretory K channels in CCD. *Am J Physiol Renal Physiol* 282: F680–F686, 2002.
43. **Woda CB, Leite M Jr, Rohatgi R, and Satlin LM.** Effects of luminal flow and nucleotides on  $[\text{Ca}^{2+}]_i$  in rabbit cortical collecting duct. *Am J Physiol Renal Physiol* 283: F437–F446, 2002.
44. **Woda CB, Miyawaki N, Ramalakshmi S, Ramkumar M, Rojas R, Zavilowitz B, Kleyman TR, and Satlin LM.** Ontogeny of flow-stimulated potassium secretion in rabbit cortical collecting duct: functional and molecular aspects. *Am J Physiol Renal Physiol* 285: F629–F639, 2003.
45. **Yip KP.** Coupling of vasopressin-induced intracellular  $\text{Ca}^{2+}$  mobilization and apical exocytosis in perfused rat kidney collecting duct. *J Physiol* 538: 891–899, 2002.